

A systematic study for the connection between hadron and its quark component nuclear modification factors

An-Ke Lei¹, Dai-Mei Zhou^{1,*}, Yu-Liang Yan^{2,*}, Du-Juan Wang³,
Xiao-Mei Li², Gang Chen⁴, Xu Cai¹ and Ben-Hao Sa^{1,2,*}

¹ Key Laboratory of Quark and Lepton Physics (MOE) and Institute of Particle Physics, Central China Normal University, Wuhan 430079, People's Republic of China

² China Institute of Atomic Energy, P. O. Box 275 (10), Beijing 102413, People's Republic of China

³ Department of Physics, Wuhan University of Technology, Wuhan 430070, People's Republic of China

⁴ Physics Department, China University of Geoscience, Wuhan 430074, People's Republic of China

E-mail: zhoum@mail.ccnu.edu.cn, yanyl@ciae.ac.cn, and sabh@ciae.ac.cn

Abstract. We have systematically studied the connection between hadron and its quark component nuclear modification factors and the flavor (mass) ordering at both parton and hadron levels in the nucleus-nucleus collisions at the LHC energies by the PACIAE model. It turns out that these two physical phenomena explored in our last publication (J. Phys. G 49 065104, 2022) are generally held, irrespective of the rapidity, centrality, reaction energy, and the collision system size. The mass ordering at hadron level in nuclear modification factor seems to be really existed, which should be studied further both theoretically and experimentally.

Keywords: heavy-ion collision, PACIAE model, nuclear modification factor

Submitted to: *J. Phys. G: Nucl. Part. Phys.*

1. Introduction

The hot and dense Quark-Gluon Plasma (QGP), a phase of deconfined matter, has been found to be created in ultra-relativistic heavy-ion collisions at both the Relativistic Heavy Ion Collider (RHIC) [1, 2, 3, 4] and the Large Hadron Collider (LHC) [5, 6, 7, 8, 9]. One of the most important signatures for QGP formation is the suppression of hadron production at high transverse momentum (p_T) due to the energy loss (jet quenching) [10, 11]. To quantify such suppression, the nuclear modification factor was proposed [12]. It is defined as the ratio of the p_T -differential multiplicities dN/dp_T in nucleus-nucleus collisions (AA) to that in the nucleon-nucleon collisions (pp), scaled by the number of binary nucleon-nucleon collisions per nucleus-nucleus collisions $\langle N_{coll} \rangle$ for a given range of centrality [12, 13]

$$R_{AA}^X(p_T) = \frac{1}{\langle N_{coll} \rangle} \frac{dN_X^{AA}/dp_T}{dN_X^{pp}/dp_T}, \quad (1)$$

where X stands for a specific particle, $\langle N_{coll} \rangle$ can be obtained from the optical Glauber model and/or the Monte-Carlo Glauber model [14, 15, 16, 17, 18, 19]. The value of R_{AA} would be unity if an AA collision is just a simple superposition of the pp collisions. Conversely, one could expect a non-unity R_{AA} in the presence of the cold and hot nuclear medium effects. Therefore, R_{AA} could serve as an excellent observable for exploring the jet quenching effect.

The R_{AA} of partons in the final partonic state (FPS) is responsible for the QGP medium-induced parton energy loss during the formation and evolution processes of QGP. On the other hand, the R_{AA} of hadrons in the final hadronic state (FHS), the one actually measurable in experiments, is the sum of partonic jet quenching above and the hadronic energy loss in hadronization and hadronic rescattering stages. Naturally, one would seek the connection between the R_{AA} of partons in FPS and the R_{AA} of hadrons in FHS. One should talk about this connection in specifics rather than in general. Taking R_{AA} of Λ as an example, the connection between R_{AA} of Λ and that of its constituent quarks could be considered in simple forms as follow:

- (a) connect R_{AA}^Λ to single R_{AA}^u (R_{AA}^d , R_{AA}^s);
- (b) connect R_{AA}^Λ to R_{AA}^{u+d} (R_{AA}^{u+s} , R_{AA}^{d+s}), calculated by the sum of u - and d - (u - and s -, d - and s -) quark p_T -distribution without weight factor;
- (c) connect R_{AA}^Λ to R_{AA}^{u+d+s} , calculated by the sum of u -, d -, and s -quark p_T -distribution without weight factor.

However, all of them are incomplete:

- (a) the d - and s - (u - and s -, u - and d -) constituent quarks are ignored;
- (b) the s - (d -, u -) constituent quark is excluded;
- (c) the contribution of sea quark s is underestimated.

As far as we know, such a connection is unable to be introduced from the first principle theory, even from the recombination (coalescence) model [20, 21, 22, 23, 24], because of the complication in dealing with the flavor composition of constituent quarks. Recently, such a connection between the hadron R_{AA} (in FHS) and its quark component one (in FPS) has been proposed by us for the first time [25], and the R_{AA} mass ordering at hadron level, initiating from the dead-cone effect [26], is also explored [25]. In this work, we extend the study to the rapidity, centrality, reaction energy, and the collision system size dependences of above two physical phenomena.

The paper is organized as follows. In section 2, the method of physical deduction of the R_{AA} correspondence between hadron and its quark component as well as the numerical framework for event generation are described. In section 3, how the above two physical phenomena depending on the rapidity, centrality, reaction energy and the collision system size is presented. We summarize in section 4.

2. Method

In this work, we follow the formalism of the correspondence between the hadron R_{AA}^h in FHS and its quark component R_{AA}^{h-q} (the script $h-q$ refers to the quark component of the hadron h) in FPS established in reference [25]. The brief physical deduction is described as follows:

Considering the hadron normalized p_T -differential distribution

$$\frac{1}{N_h} dN_h/dp_T,$$

its corresponding quark component normalized p_T -differential distribution is

$$\frac{1}{N_{h-q}} \sum_q \frac{1}{N_q} dN_q/dp_T.$$

In the above expressions, N_h (N_q) refers to the multiplicity of the hadron h (quark q). N_{h-q} denotes the number of constituent quarks in a hadron h and the sum is taken over all constituent quarks.

Multiplying above two expressions by N_h , one can get the hadron un-normalized p_T -differential distribution

$$dN_h/dp_T$$

and the corresponding quark component un-normalized p_T -differential distribution

$$\frac{1}{N_{h-q}} \sum_q \frac{N_h}{N_q} dN_q/dp_T.$$

Substituting above two un-normalized p_T -differential distributions into equation (1), respectively, one obtains the hadron nuclear modification factor

$$R_{AA}^h(p_T) = \frac{1}{\langle N_{coll} \rangle} \frac{dN_h^{AA}/dp_T}{dN_h^{pp}/dp_T}, \quad (2)$$

and its corresponding quark component nuclear modification factor

$$R_{AA}^{h-q}(p_T) = \frac{1}{\langle N_{coll} \rangle} \frac{\sum_q w_q^{AA} dN_q^{AA}/dp_T}{\sum_q w_q^{pp} dN_q^{pp}/dp_T}, \quad (3)$$

where $w_q = N_h/N_q$ is the weight factor.

To investigate the correspondence between hadron and its quark component and the mass ordering at hadron level in R_{AA} , a numerical Monte-Carlo event generator, PACIAE [27], is employed to simulate the pp and AA collisions. PACIAE is a microscopic parton and hadron cascade model based on but beyond the PYTHIA6.4 event generator [28].

For nucleon-nucleon (NN) collisions, with respect to PYTHIA, the partonic and hadronic rescatterings are introduced before and after the hadronization, respectively. The final hadronic state is developed from the initial partonic hard scattering and parton showers, followed by parton rescattering, string fragmentation, and hadron rescattering stages. Thus, the PACIAE model provides a multi-stage transport description on the evolution of the collision system.

For AA collisions, the initial positions of nucleons in the colliding nuclei are sampled according to the Woods-Saxon distribution. Together with the initial momentum setup of $p_x = p_y = 0$ and $p_z = p_{\text{beam}}$ for each nucleon, a list containing the initial state of all nucleons in a given AA collision is constructed. A collision happened between two nucleons from different nuclei if their relative transverse distance is less than or equal to the minimum approaching distance: $D \leq \sqrt{\sigma_{\text{NN}}^{\text{tot}}/\pi}$. The collision time is calculated with the assumption of straight-line trajectories. All such nucleon pairs compose an NN collision time list. An NN collision with least collision time is selected from the list and executed by PYTHIA (PYEVNW subroutine) with the hadronization temporarily turned-off, as well as the strings and diquarks broken-up. The nucleon list and NN collision time list are then updated. A new NN collision with least collision time is selected from the updated NN collision time list and executed by PYTHIA. With repeating the aforementioned steps till the NN collision list empty, the initial partonic state is constructed for a AA collision.

Then, the partonic rescatterings are performed, where the LO-pQCD parton-parton cross section [29, 30] is employed. After partonic rescattering, the string is recovered and then hadronized with the Lund string fragmentation scheme resulting in an intermediate hadronic state. Finally, the system proceeds into the hadronic rescattering stage and produces the final hadronic state observed in the experiments.

Thus PACIAE Monte-Carlo simulation provides a complete description of the NN and/or AA collisions, which includes the partonic initialization stage, partonic rescattering stage, hadronization stage, and the hadronic rescattering stage. Meanwhile, the PACIAE model simulation could be selected to stop at any stages desired conveniently. In this work, the simulations are stopped at the final partonic state (FPS) after partonic rescattering or at final hadronic state (FHS) after hadronic rescattering

for the calculations of R_{AA}^h and R_{AA}^{h-q} , respectively. More details could be found in the reference [27].

In order to maintain self-consistency, the tuning parameters are kept consistent with those in reference [25]: a factor multiplying on the hard scattering cross-section $K=2.7$ (0.7), the Lund string fragmentation parameters of $\alpha=1.3$ (0.1) and $\beta=0.09$ (0.58), as well as the Gaussian width of the primary hadron transverse momentum distribution $\omega=0.575$ (0.36) are implemented in AA (pp) simulations.

3. Results and discussions

In reference [25], we have proposed a method connecting the hadron nuclear modification factor R_{AA}^h in FHS to its quark component nuclear modification factor R_{AA}^{h-q} in FPS, and explored the mass ordering in R_{AA}^h at hadron level in the 0-5% most central Pb+Pb collisions at $\sqrt{S_{NN}}=2.76$ TeV. In this section, we will expand our research discussing their dependences on rapidity, centrality, reaction energy, and the collision system size. Our simulations are all performed in full η phase space, except those in section 3.1.

3.1. Rapidity dependence

Figure 1 shows the meson R_{AA} in FHS (black solid circles) and its quark component R_{AA} in FPS (red open circles) within different η ranges in the 0-5% most central Pb+Pb collisions at $\sqrt{S_{NN}}=2.76$ TeV. From top to bottom rows are R_{AA} of $\pi^+(u\bar{d})$, $K^+(u\bar{s})$ and $\phi^0(s\bar{s})$, while from left to right columns are those in $|\eta| < 0.8$, 2.5 and full η phase space[‡]. Figure 2 shows the same content, just for the baryon sector. A peak appears at p_T around $1 \sim 2$ GeV/c, which is the so-called Cronin effect [31] attributed to the multiple initial-state scattering of partons [32]. In figures 1 and 2, one can see the correspondence between hadron R_{AA} and its quark component R_{AA} maintains well in all three rapidity ranges. The meson and baryon R_{AA} are smaller than their quark component R_{AA} above $p_T \sim 2$ GeV/c, even in the midrapidity of $|\eta| < 0.8$, due to more radiation and collision energy losses the hadron suffered than the ones of its quark component. Moreover, this discrepancy becomes more pronounced as the η range increases. This is because the energy loss increases with the increasing number of colliding and radiating particles involved in a wider η range.

In figure 3, we compare the flavor (mass) ordering of the quarks (in FPS), mesons (in FHS), and the baryons (in FHS) nuclear modification factors among three different η phase spaces, as displayed from left to right column, respectively. For quark sector, a nearly flat R_{AA} of the heavy c -quark is observed. This could be understood from the fact that the c -quark is produced in initial hard processes and transparent in the partonic and hadronic rescatterings. Hence the p_T distribution of c -quark in Pb+Pb collisions is approximately parallel to that in p+p collisions at

[‡] Such a graph arrangement manner would also be utilized hereafter, just for different particle sectors and conditions applied.

the same energy. The flavor (mass) ordering seems to be generally held for quarks and mesons. However, for baryons, it seems to be recognizable only in full η phase space. This can be explained by the relative mass discrepancy among selected observing particles in the three categories above. The relative mass discrepancy among baryons ($m_p \approx 0.938$ GeV, $m_{\Lambda^0} \approx 1.116$ GeV and $m_{\Xi^-} \approx 1.322$ GeV [33]) is smaller than that of the mesons ($m_{\pi^+} \approx 140$ MeV, $m_{K^+} \approx 494$ MeV and $m_{\phi^0} \approx 1.02$ GeV) and is much smaller than the one of the quarks ($m_u \approx 2.2$ MeV, $m_s \approx 93$ MeV and $m_c \approx 1.27$ GeV).

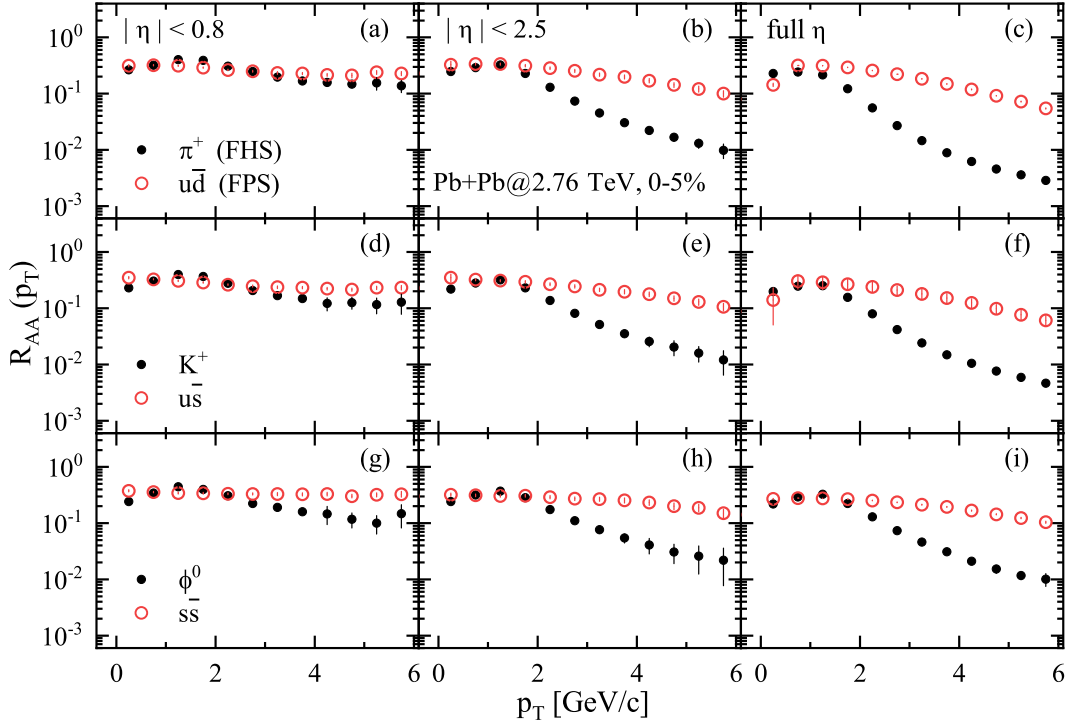


Figure 1. The nuclear modification factors of mesons (in FHS, black solid circles) and their quark component (in FPS, red open circles) in the 0-5% most central Pb+Pb collisions at $\sqrt{S_{NN}}=2.76$ TeV within three pseudo-rapidity ranges.

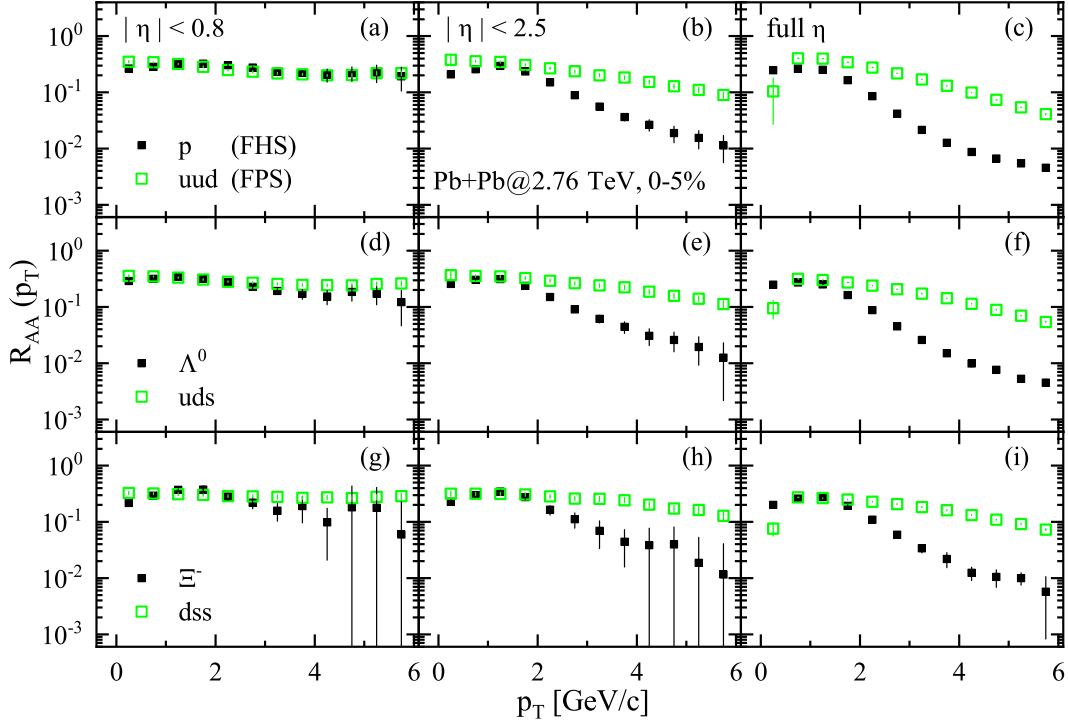


Figure 2. The nuclear modification factors of baryons (in FHS, black solid squares) and their quark component (in FPS, green open squares) in the 0-5% most central Pb+Pb collisions at $\sqrt{s_{NN}}=2.76$ TeV within three pseudo-rapidity ranges.

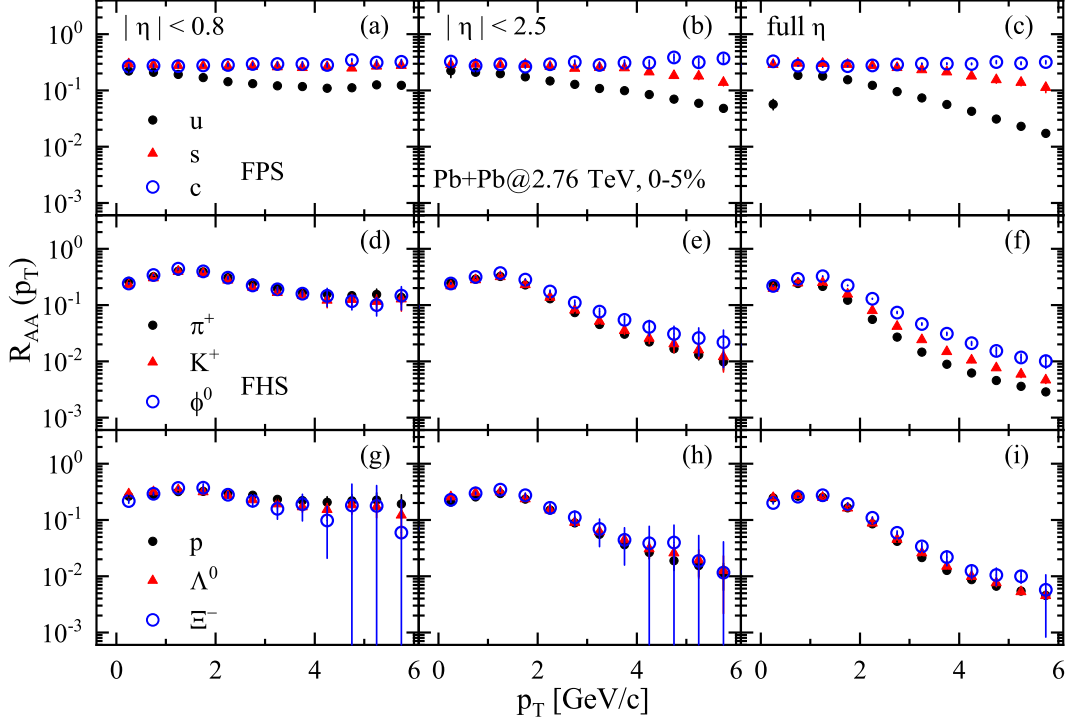


Figure 3. The nuclear modification factors of quarks (in FPS), mesons (in FHS) and baryons (in FHS) in the 0-5% most central Pb+Pb collisions at $\sqrt{s_{NN}}=2.76$ TeV within three pseudo-rapidity ranges.

3.2. Centrality dependence

In figure 4 and figure 5, we show hadron (meson and baryon in FHS) R_{AA} and its quark component R_{AA} (in FPS) in 0-5%, 5-20% and 20-60% centrality classes of Pb+Pb collisions at $\sqrt{S_{NN}}=2.76$ TeV. Still, the physical phenomenon of the correspondence between hadron and its quark component nuclear modification factors as well as the hadron R_{AA} less than its quark component R_{AA} is keeping in all of the three centrality classes. One can see approximately a more depressed magnitude of both R_{AA} in more central centrality class stemming from a stronger hot medium effect. Nevertheless, the discrepancy between hadron R_{AA} and its quark component R_{AA} brought about by centrality classes is not so significant.

Meanwhile, in figure 6 we give the simulated R_{AA} of quarks (in FPS), mesons (in FHS) and baryons (in FHS) in 0-5%, 5-20%, and 20-60% centralities of Pb+Pb collisions at $\sqrt{S_{NN}}=2.76$ TeV. The good flavor (mass) ordering in the region of $p_T > 2$ GeV/c is generally held. However, the ordering extent changing with centrality is insensitive.

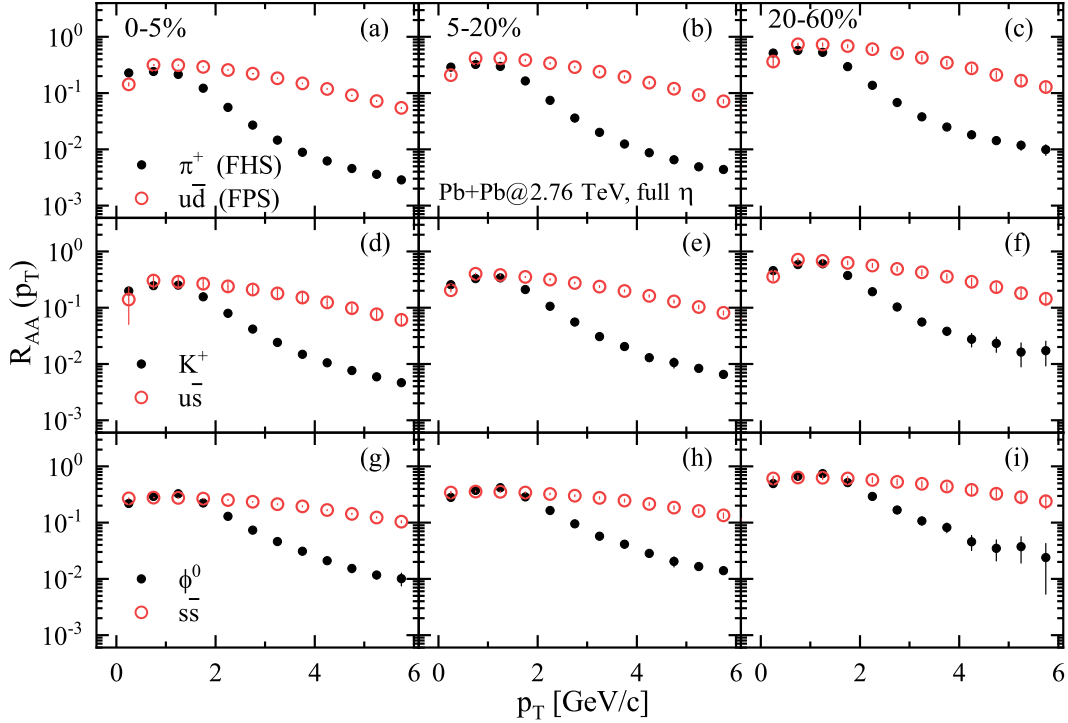


Figure 4. The nuclear modification factors of mesons (in FHS, black solid circles) and their quark component (in FPS, red open circles) in the different centrality classes of Pb+Pb collisions at $\sqrt{S_{NN}}=2.76$ TeV.

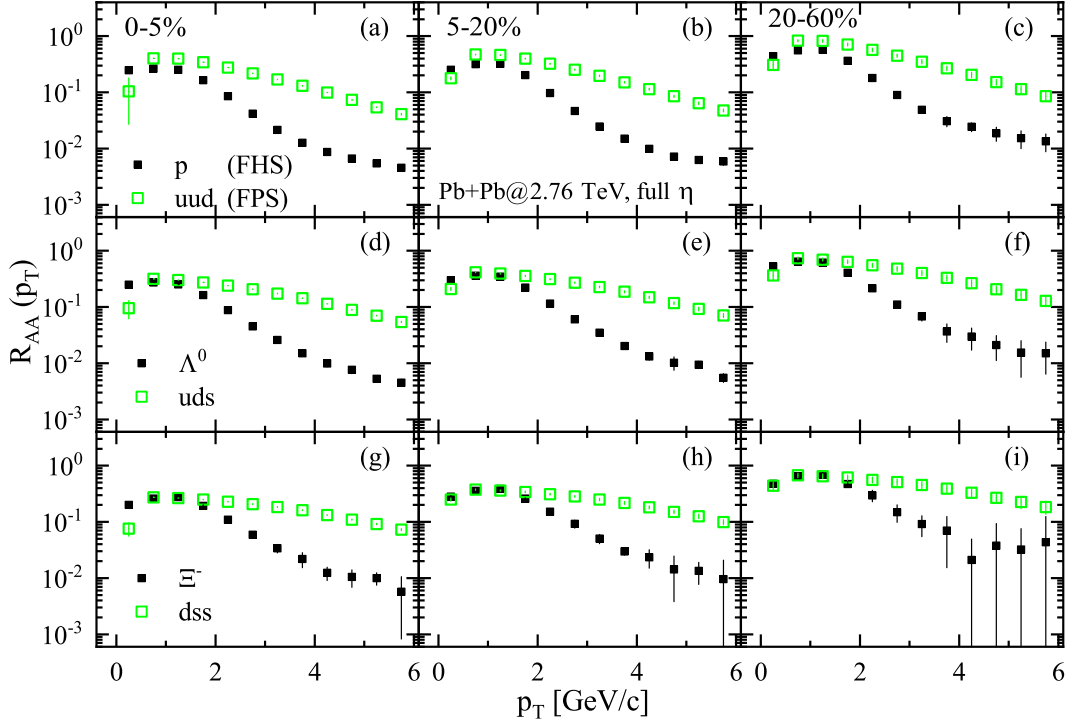


Figure 5. The nuclear modification factors of baryons (in FHS, black solid squares) and their quark component (in FPS, green open squares) in the different centrality classes of Pb+Pb collisions at $\sqrt{s_{NN}}=2.76$ TeV.

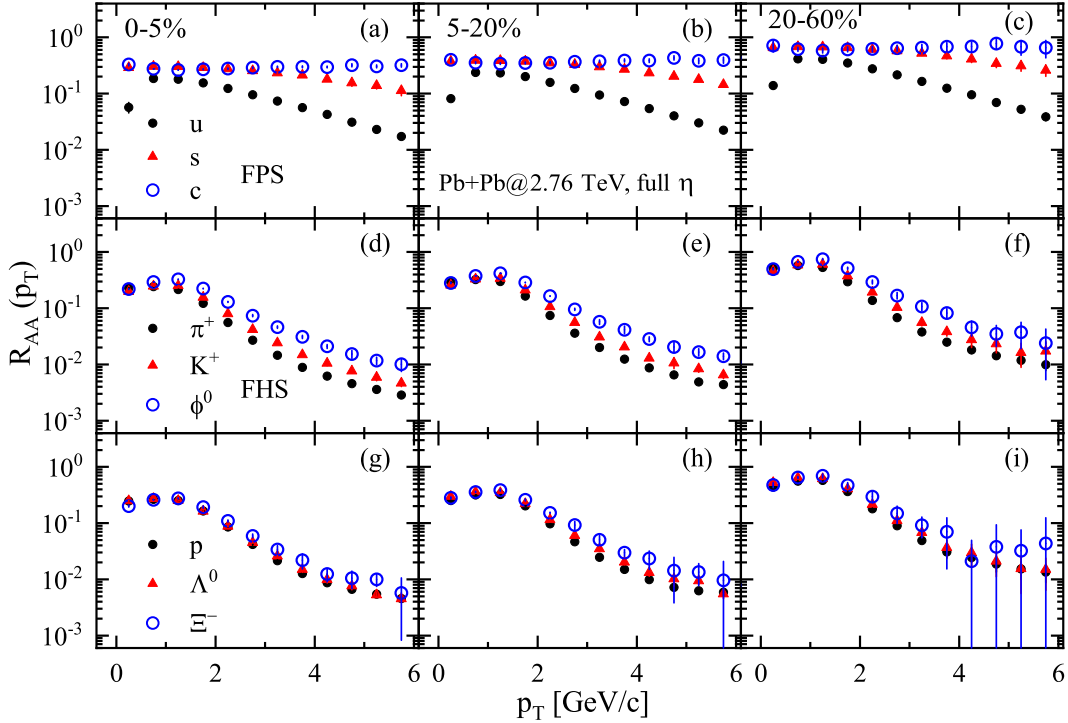


Figure 6. The nuclear modification factors of quarks (in FPS), mesons (in FHS), and baryons (in FHS) in the different centrality classes of Pb+Pb collisions at $\sqrt{s_{NN}}=2.76$ TeV.

3.3. Energy dependence

We now study the energy dependence of the two physical phenomena: the correspondence between hadron R_{AA} and its quark component one, and the flavor (mass) ordering at both the parton and hadron levels. In figure 7 and 8, we give the R_{AA} of both the hadrons (in FHS) and their quark component (in FPS) in 0-5% most central Pb+Pb at $\sqrt{S_{NN}}=0.9, 2.76$ and 5.02 TeV. The physical phenomenon of correspondence is kept well at all three reaction energies. However, the discrepancy of R_{AA} between hadron and its quark component is not varied strongly with the collision energies.

In figure 9 the flavor (mass) ordering at both the parton and hadron levels are given. Here we can see the mass ordering at hadron level appears in all three reaction energies, like the one at parton level. However, it seems also showing the mass ordering at both of parton and hadron levels is more pronounced at the lower energy rather than the higher one. It should be studied further.

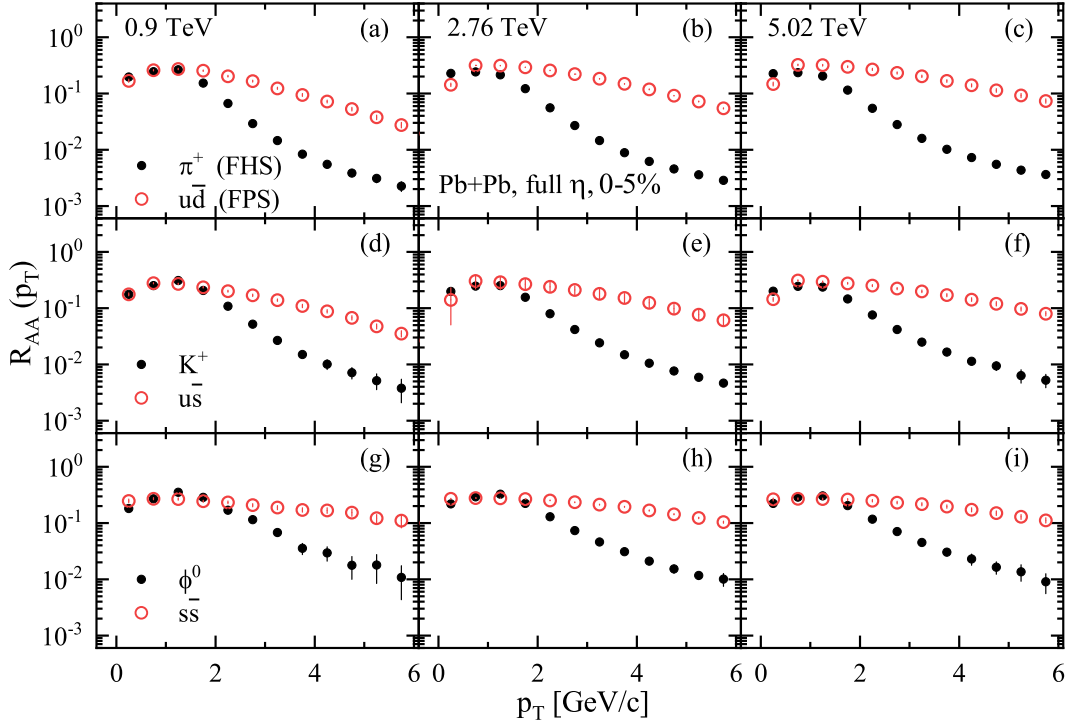


Figure 7. The nuclear modification factors of mesons (in FHS, black solid circles) and their quark component (in FPS, red open circles) in the 0-5% most central Pb+Pb collisions at different reaction energies.

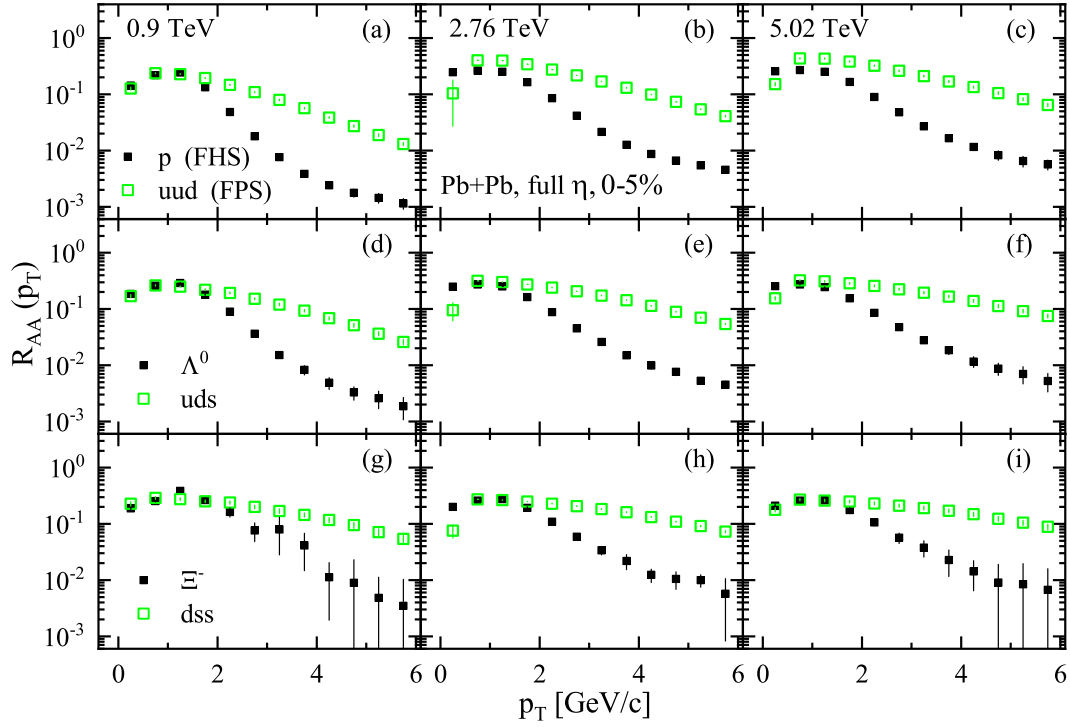


Figure 8. The nuclear modification factors of baryons (in FHS, black solid squares) and their quark component (in FPS, green open squares) in the 0-5% most central Pb+Pb collisions at different reaction energies.

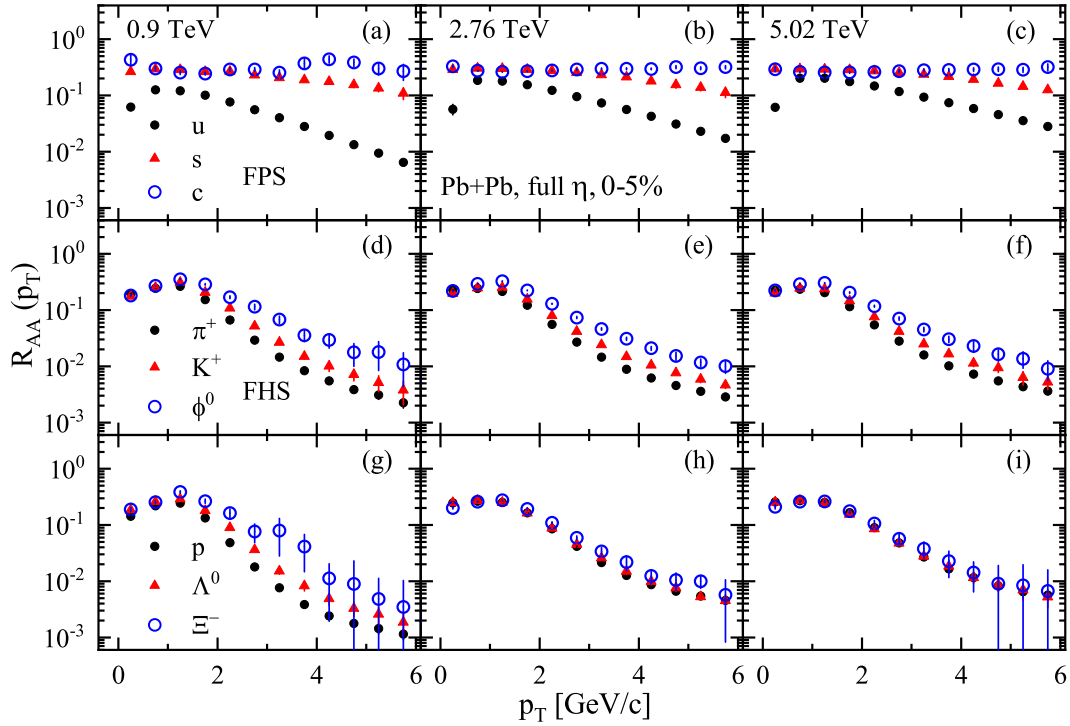


Figure 9. The nuclear modification factors of quarks (in FPS), mesons (in FHS), and baryons (in FHS) in the 0-5% most central Pb+Pb collisions at different reaction energies.

3.4. System size dependence

In figure 10 (meson) and figure 11 (baryon), we compare the hadron R_{AA} with its quark component one in the 0-5% most central Cu+Cu, Xe+Xe and Pb+Pb collisions at $\sqrt{S_{NN}}=2.76$ TeV. We present the mass ordering at both the parton and hadron levels for the same reaction systems above in figure 12. These figures show again that, the physical phenomena of the correspondence between hadron and its quark component as well as the flavor (mass) ordering are well kept.

As the amount of interacting matter increases with the system size increasing, the particle propagating length is longer in larger collision system size. Hence the larger the system size, the more energy losses there are [34]. Consequently, the R_{AA} would decrease with the collision system size increasing, as shown in figure 10, 11 and 12 from left to right.

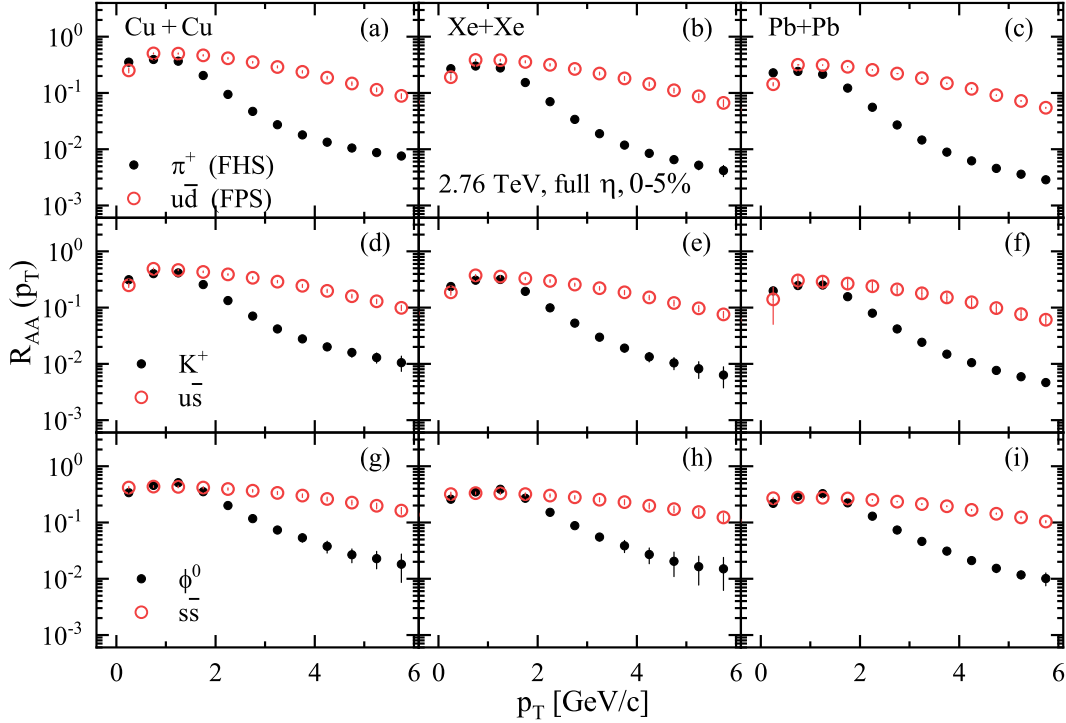


Figure 10. The nuclear modification factors of mesons (in FHS, black solid circles) and their quark component (in FPS, red open circles) in the 0-5% most central Cu+Cu, Xe+Xe and Pb+Pb collisions at $\sqrt{S_{NN}}=2.76$ TeV.

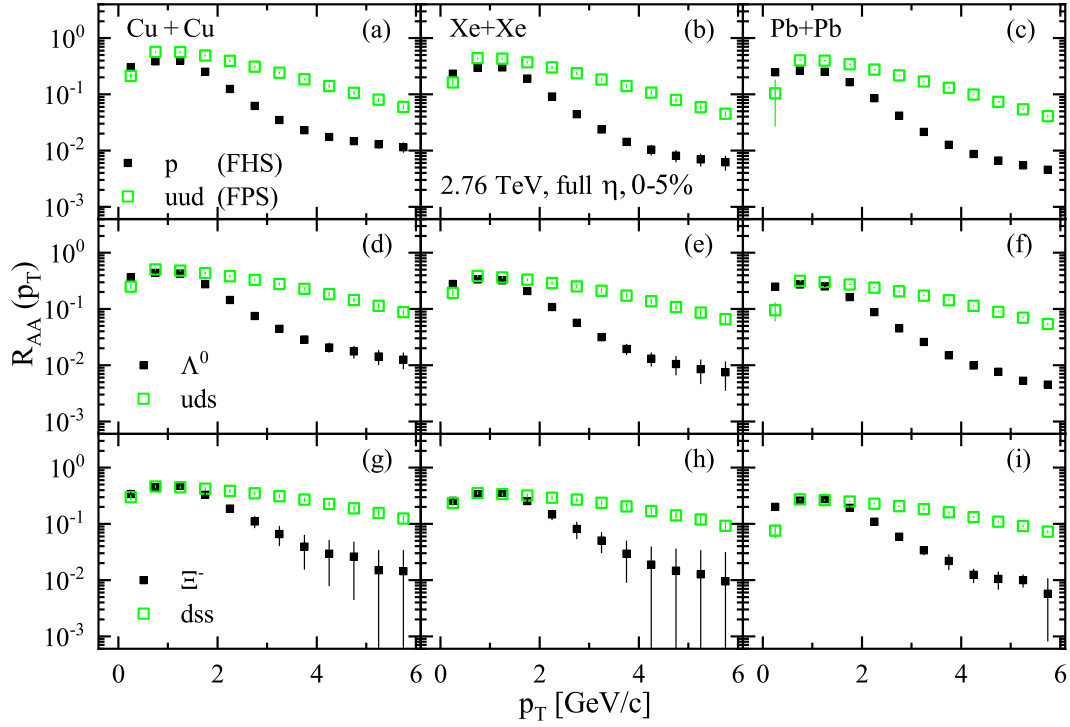


Figure 11. The nuclear modification factors of baryons (in FHS, black solid squares) and their quark component (in FPS, green open squares) in the 0-5% most central Cu+Cu, Xe+Xe and Pb+Pb collisions at $\sqrt{s_{NN}} = 2.76$ TeV.

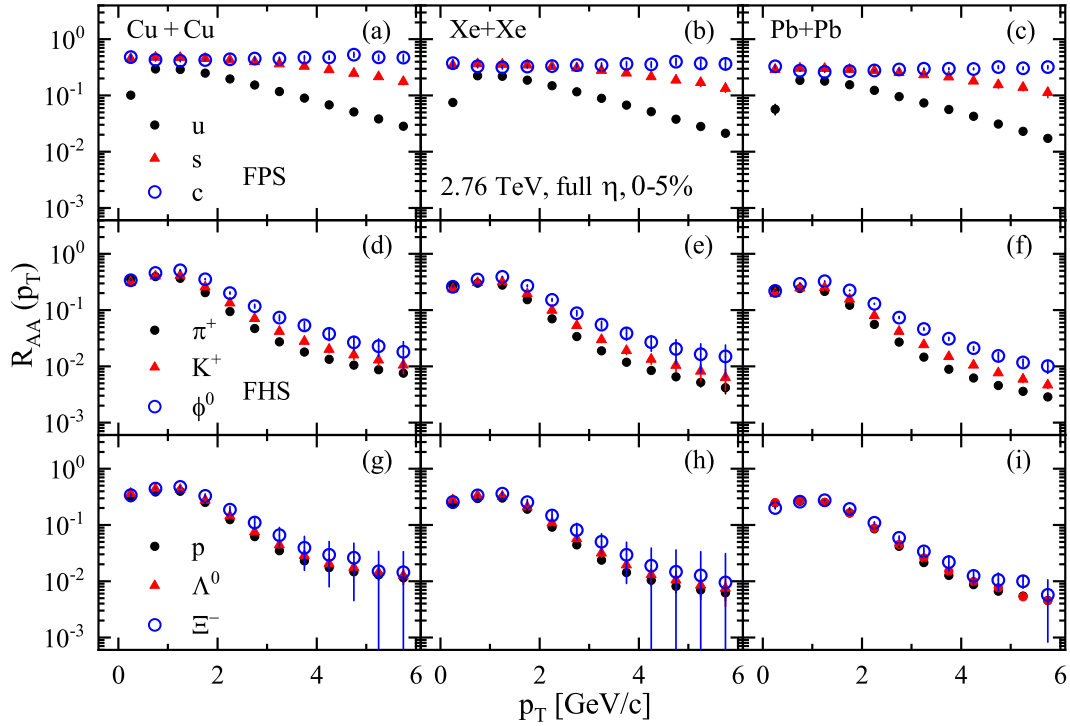


Figure 12. The nuclear modification factors of quarks (in FPS), mesons (in FHS), and baryons (in FHS) in the 0-5% most central Cu+Cu, Xe+Xe and Pb+Pb collisions at $\sqrt{s_{NN}} = 2.76$ TeV.

4. Summary

In summary, via the parton and hadron cascade model PACIAE, we study the correspondence between hadron nuclear modification factor and its quark component one, as well as the flavor (mass) ordering at both parton and hadron levels. Meanwhile, how the above two physical phenomena change with the (pseudo-)rapidity, centrality, reaction energy and the collision system size are all investigated systematically.

Generally speaking, the correspondence between hadron and its quark component and the mass ordering at hadron level in nuclear modification factors are held, irrespective of the rapidity, centrality, reaction energy, and the collision system size.

For the correspondence, the R_{AA} of the hadron is always less than that of its quark component in the p_T region above 2 GeV/c. The discrepancy between them becomes more pronounced in a wider η range. However, the centrality, reaction energy and the system size do not show noticeable influence on it. The flavor (mass) ordering is easier to distinguish in the wider η and the lower reaction energy, while this observation does not clearly exhibit in the dependence of centrality and/or the collision system size.

The mass ordering in nuclear modification factor at hadron level, like the one at parton level, seems to be existed really. Its clear observation is relevant to the relative discrepancy among the selected candidates in mass. The larger the relative discrepancy among those candidates in mass, the clearer mass ordering is observed.

Of course, the correspondence between hadron and its quark component and the hadronic mass ordering in the nuclear modification factor should be studied further, both theoretically and experimentally. In the next study, we would consider the open-charm and/or the open-bottom heavy-hadron [35] as the candidates.

Acknowledgments

We thank C. B. Yang for discussions. This work was supported by the National Natural Science Foundation of China (11775094, 11905188, 11775313, 11905163), the Continuous Basic Scientific Research Project (No.WDJC-2019-16), National Key Research and Development Project (2018YFE0104800) and by the 111 project of the foreign expert bureau of China.

References

- [1] Adcox K *et al.* (PHENIX) 2005 *Nucl. Phys. A* **757** 184–283 (*Preprint nucl-ex/0410003*)
- [2] Arsene I *et al.* (BRAHMS) 2005 *Nucl. Phys. A* **757** 1–27 (*Preprint nucl-ex/0410020*)
- [3] Back B B *et al.* (PHOBOS) 2005 *Nucl. Phys. A* **757** 28–101 (*Preprint nucl-ex/0410022*)
- [4] Adams J *et al.* (STAR) 2005 *Nucl. Phys. A* **757** 102–183 (*Preprint nucl-ex/0501009*)
- [5] Aamodt K *et al.* (ALICE) 2010 *Phys. Rev. Lett.* **105** 252302 (*Preprint 1011.3914*)
- [6] Aad G *et al.* (ATLAS) 2010 *Phys. Rev. Lett.* **105** 252303 (*Preprint 1011.6182*)
- [7] Aamodt K *et al.* (ALICE) 2011 *Phys. Lett. B* **696** 30–39 (*Preprint 1012.1004*)
- [8] Chatrchyan S *et al.* (CMS) 2011 *Phys. Rev. C* **84** 024906 (*Preprint 1102.1957*)
- [9] Abelev B *et al.* (ALICE) 2012 *Phys. Rev. Lett.* **109** 072301 (*Preprint 1202.1383*)

- [10] Bjorken J D 1982 Energy Loss of Energetic Partons in Quark-Gluon Plasma: Possible Extinction of High p_T Jets in Hadron-Hadron Collisions Tech. Rep. FERMILAB-PUB-82-059-T FERMILAB URL <http://lss.fnal.gov/archive/preprint/fermilab-pub-82-059-t.shtml>
- [11] Gyulassy M and Plumer M 1990 *Phys. Lett. B* **243** 432–438
- [12] Wang X N 1998 *Phys. Rev. C* **58** 2321 (*Preprint hep-ph/9804357*)
- [13] Klein-Bösing C (ALICE) 2018 *PoS LHCP2018* 222 (*Preprint 1809.04936*)
- [14] Glauber R J and Matthiae G 1970 *Nucl. Phys. B* **21** 135–157
- [15] Miller M L, Reygers K, Sanders S J and Steinberg P 2007 *Ann. Rev. Nucl. Part. Sci.* **57** 205–243 (*Preprint nucl-ex/0701025*)
- [16] Abelev B I *et al.* (STAR) 2009 *Phys. Rev. C* **79** 034909 (*Preprint 0808.2041*)
- [17] Abelev B *et al.* (ALICE) 2013 *Phys. Rev. C* **88** 044909 (*Preprint 1301.4361*)
- [18] Loizides C, Nagle J and Steinberg P 2015 *SoftwareX* **1-2** 13–18 (*Preprint 1408.2549*)
- [19] Loizides C, Kamin J and d’Enterria D 2018 *Phys. Rev. C* **97** 054910 [Erratum: *Phys.Rev.C* 99, 019901 (2019)] (*Preprint 1710.07098*)
- [20] Hwa R C and Yang C B 2003 *Phys. Rev. C* **67** 034902 (*Preprint nucl-th/0211010*)
- [21] Greco V, Ko C M and Levai P 2003 *Phys. Rev. Lett.* **90** 202302 (*Preprint nucl-th/0301093*)
- [22] Greco V, Ko C M and Levai P 2003 *Phys. Rev. C* **68** 034904 (*Preprint nucl-th/0305024*)
- [23] Fries R J, Muller B, Nonaka C and Bass S A 2003 *Phys. Rev. Lett.* **90** 202303 (*Preprint nucl-th/0301087*)
- [24] Fries R J, Muller B, Nonaka C and Bass S A 2003 *Phys. Rev. C* **68** 044902 (*Preprint nucl-th/0306027*)
- [25] Sa B H, Zhou D M, Yan Y L, Liu W D, Hu S Y, Li X M, Zheng L, Chen G and Cai X 2022 *J. Phys. G* **49** 065104
- [26] Dokshitzer Y L, Khoze V A and Troian S I 1991 *J. Phys. G* **17** 1602–1604
- [27] Sa B H, Zhou D M, Yan Y L, Li X M, Feng S Q, Dong B G and Cai X 2012 *Comput. Phys. Commun.* **183** 333–346 (*Preprint 1104.1238*)
- [28] Sjostrand T, Mrenna S and Skands P Z 2006 *JHEP* **05** 026 (*Preprint hep-ph/0603175*)
- [29] Combridge B L, Kripfganz J and Ranft J 1977 *Phys. Lett. B* **70** 234
- [30] Field R D 1989 *Applications Of Perturbative QCD* (Addison-Wesley Publishing Company, Inc.)
- [31] Cronin J W, Frisch H J, Shochet M J, Boymond J P, Mermod R, Piroue P A and Sumner R L (E100) 1975 *Phys. Rev. D* **11** 3105–3123
- [32] Wang X N 2000 *Phys. Rev. C* **61** 064910 (*Preprint nucl-th/9812021*)
- [33] Zyla P A *et al.* (Particle Data Group) 2020 *PTEP* **2020** 083C01
- [34] Wang X N 2005 *Nucl. Phys. A* **750** 98–120 (*Preprint nucl-th/0405017*)
- [35] Andronic A *et al.* 2016 *Eur. Phys. J. C* **76** 107 (*Preprint 1506.03981*)